RELAP5/MOD3.2 Assessment Using INSC SP-V7

Paul D. Bayless, INEEL
Mikhail V. Davydov, EREC

April 2002

Abstract

Assessments of the RELAP5/MOD3.2 computer code using critical heat flux data from three sets of experiments have been performed independently by analysts at the Electrogorsk Research and Engineering Center and the Idaho National Engineering and Environmental Laboratory. The experiments, performed at the KS-1 and V-200 facilities, investigated dryout at the top of rod bundles with geometry typical of VVER reactors. The two assessments were compared, investigating differences in the input models and explaining the resultant differences in the calculations. The differences between the two sets of calculations were generally much smaller than the differences between the calculations and the data. Both assessments found that the code calculations were in minimal agreement with the data, and recommended the development of a more applicable critical heat flux model for the code. Recommendations for the input models included accurately describing the bundle geometry and not using the thermal front tracking model in heated bundles.

Introduction

Calculations of VVER Standard Problem V7 have been performed independently by analysts at the Electrogorsk Research and Engineering Center (EREC) and the Idaho National Engineering and Environmental Laboratory (INEEL). This standard problem represents rod bundle critical heat flux (CHF) data from three sets of experiments, two at the KS-1 facility at the Russian Research Center - Kurchatov Institute, and one set from the V-200 facility at the Institute of Physics and Power Engineering. These assessments aid in assessing the applicability of RELAP5/MOD3.2 for analyzing transients in VVER type reactors.

Test and Facility Descriptions

The KS-1 test facility is designed to study thermal hydraulic processes under normal, transient and emergency conditions in water-cooled water-moderated power reactors of the VVER type. The KS-1 is a semi-integral single loop model of the VVER primary system. The fuel assembly model for the core consists of full height electrically heated rods. Forced or natural circulation flow of the coolant can be modeled.

A large number of tests were conducted over many years in the KS-1 test facility. For standard problem INSC SP-V7, tests from 19- and 37-rod bundle experiments were selected. These rod bundles are referred to as 3/- and 4/-, respectively, and are shown in Figures 1 and 2. Both bundles had heater rods with a 2.5-m heated length. In the 37-rod bundle 4/-, the center rod was

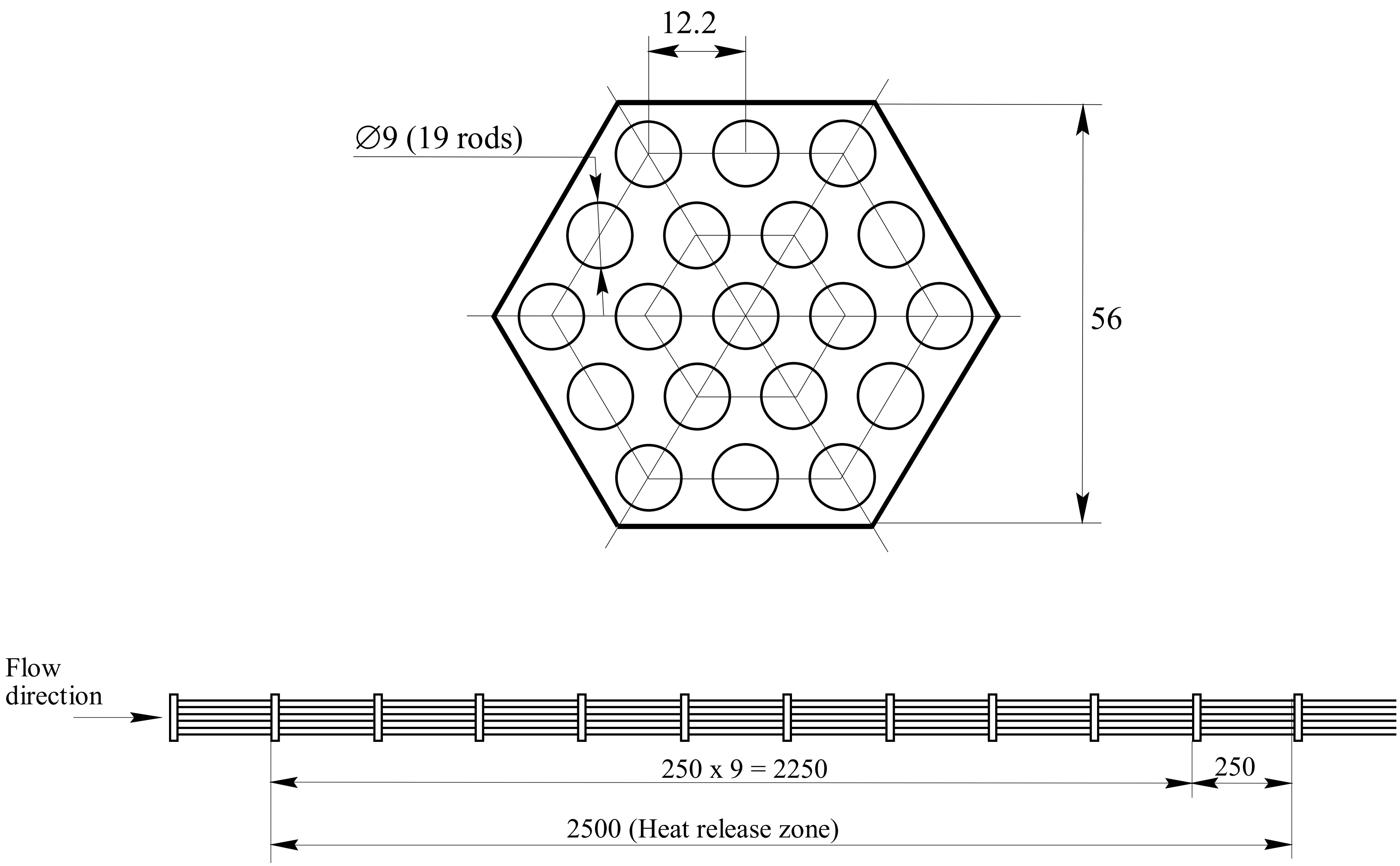

Figure 1. Geometric parameters of the KS-1 rod bundle 3/-.

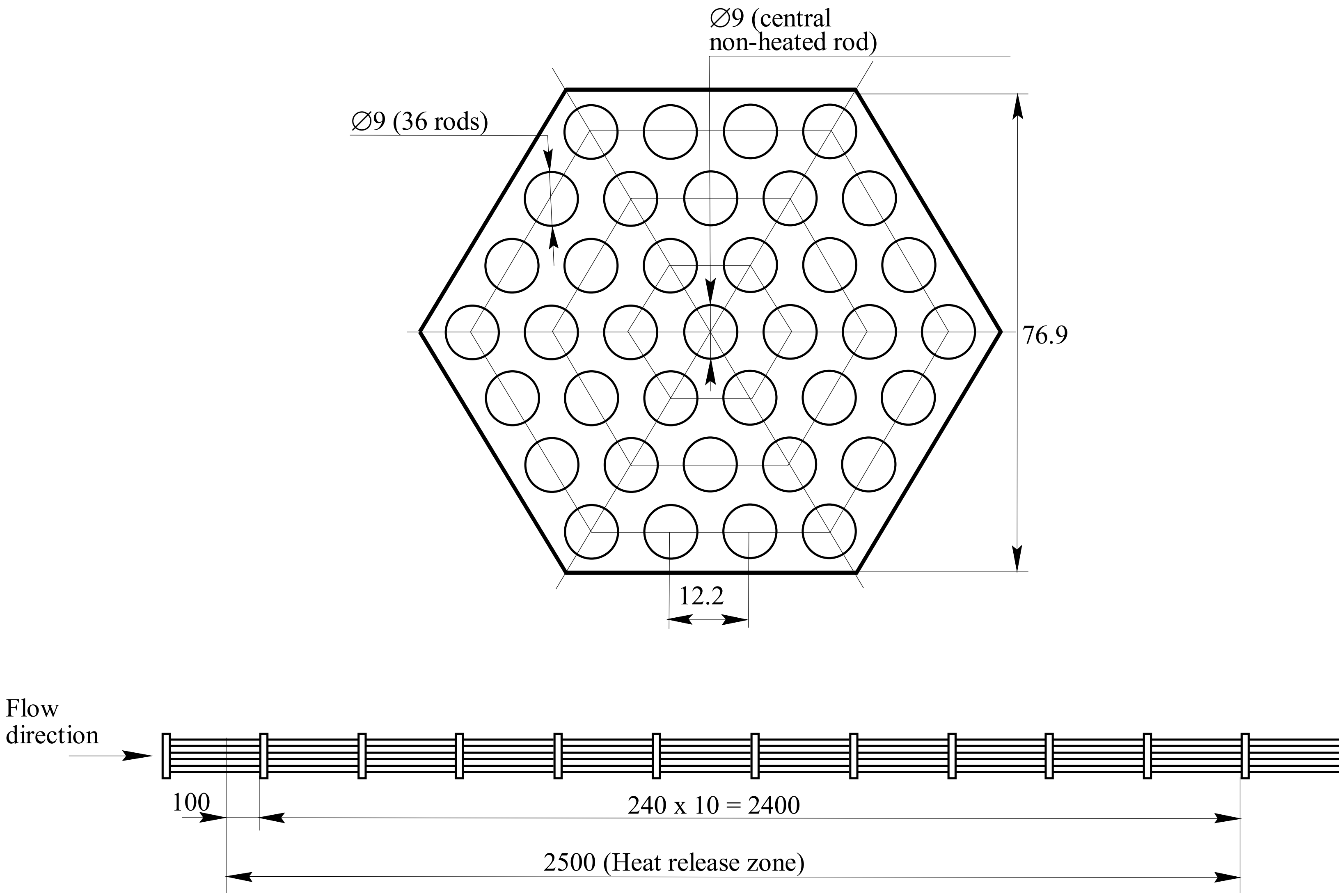

Figure 2. Geometric parameters of the KS-1 rod bundle 4/-.

unheated. The rods were made of 12X18H10T stainless steel tubes with an outer diameter of 9.0 mm and a wall thickness of 1.53 mm. The heater rod pitch was 12.2 mm. In the heated zone, there were 10 grid spacers, located every 250 mm in the 3/- bundle and every 240 mm in the 4/- bundle. The grid spacer geometry is the same as that used in VVER-440 reactors. Both bundles had uniform axial and radial power profiles, and were enclosed in hexagonal working channels.

The data selected for this standard problem represent a wide range of pressure (0.8–7.0 MPa), mass flux (220-2852 kg/m^2s), and inlet subcooling (0-205 K). The reported heat flux is the net heat flux; that is, it accounts for the heat loss from the bundle to the environment. The stated uncertainty in the measured CHF in the KS-1 facility was 10%.

The V-200 test facility is designed to study thermal hydraulic processes in circulation circuits and core components of VVER type power reactors for a wide range of fluid conditions. It is a high-pressure, forced circulation circuit made of stainless steel tubes with inside diameters up to 50 mm, and includes several loops with replaceable experimental working sections. The fuel assembly model for the core consists of reduced height electrically heated rods. Forced circulation flow of the coolant can be provided by centrifugal pumps.

The V-200 rod bundle had seven heater rods. The rods were made of 1X18H9T stainless steel tubes with an outer diameter of 9.1 mm and a wall thickness of 0.6 mm. The heater rod pitch was 12.8 mm. The heated length of the rod bundle was 800 mm. In the heated zone, the rod bundle had two grid spacers, 400 mm apart, one near the bottom and one near the middle. A third grid spacer was located just above the heated region. The grid spacer geometry is the same as that used in VVER reactors. This bundle had uniform axial and radial power profiles. The V-200 rod bundle was situated in the working channel with a complex hexagonal/triangular geometry. The cross section of the rod bundle is presented in Figure 3.

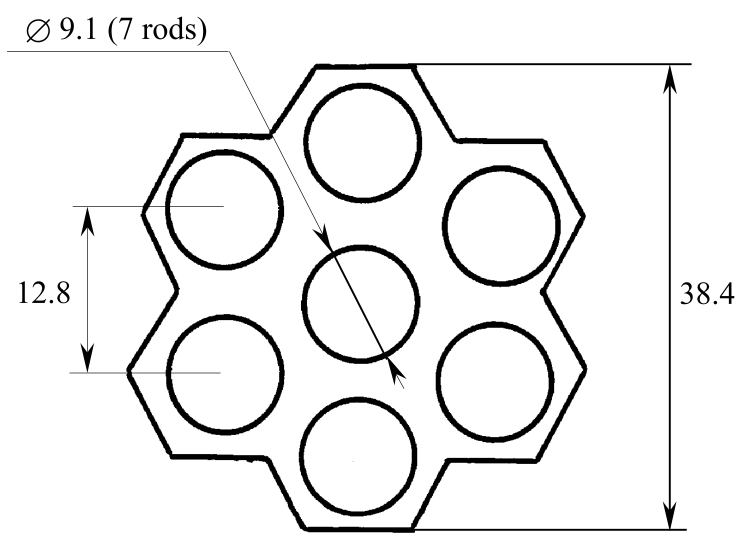

Figure 3. Cross section of the V-200 rod bundle.

The V-200 tests selected for the standard problem were all run at a pressure of 6.8 MPa, with a nominal mass flux of either 210 or 350 kg/m^{2}s. The inlet subcooling ranged from 25-211 K.

The objective of all the tests was to measure parameters at the onset of the heater rod temperature excursion following CHF. Individual tests were started with a steady state condition at the desired pressure. The CHF was approached either by holding the flow rate constant and increasing the power, or by holding the power constant and reducing the flow rate or increasing the coolant inlet temperature until elevated and increasing temperatures were measured on the heater rods.

RELAP5 Input Model Descriptions

The general nodalization scheme for the EREC rod bundle input models is shown in Figure 4. The input model consists of seven hydrodynamic components and one heat structure. The bundle inlet temperature and flow rate are established by the inlet time dependent volume and junction, respectively. A lower plenum volume is used to check the inlet pressure. The rod bundle is simulated with a pipe component, with an attached heat structure modeling the heater rods. In the input decks for the KS-1 facility, there is an unheated volume at the bottom of the bundle; this unheated volume is not included in the V-200 input deck. In all of the input decks, there was a one-to-one correspondence in the axial nodalization of the rod bundle hydrodynamic cells and the heat structure. At the top of the bundle, a single junction connected the pipe outlet to a time dependent volume, which established the pressure boundary condition. Because the data provided were for net heat flux, the outer bundle wall was not modeled.

The number of axial nodes in the pipe modeling the bundle varied between the experiment sets. For the KS-1 4/- bundle, there were 21 cells over the heated length, with grid spacers located at every second junction. For the KS-1 3/- bundle, there were 20 cells over the heated length, again with grid spacers located at every second junction. For the V-200 bundle, there were 8 cells over the heated length, with grid spacers at the bundle inlet, outlet, and mid-plane. Loss coefficients of 0.26 were used for the grid spacers.

The heater rods were modeled as cylindrical heat structures; seven mesh points were used for the KS-1 bundles, and four for the V-200 bundle. The vertical rod bundle without crossflow heat transfer package was used. The heated diameters were 10.88 mm for the KS-1 4/- bundle, 11.22 mm for the KS-1 3/- bundle, and 10.75 mm for the V-200 bundle.

Default code options were used in most cases. In the bundle, the bundle interphase drag and thermal front tracking models were turned on, and the water packing scheme was turned off. Choking was turned off at all junctions.

The same calculation procedure was used for all of the calculations. The inlet boundary conditions (pressure, temperature and mass flow rate) were set according to the current data point. Preliminary values were chosen for the outlet pressure and initial rod bundle power; this value was somewhat smaller than the critical value from the CHF data base. The calculation began with 30 s of constant power, after which the rod bundle power was slowly increased for

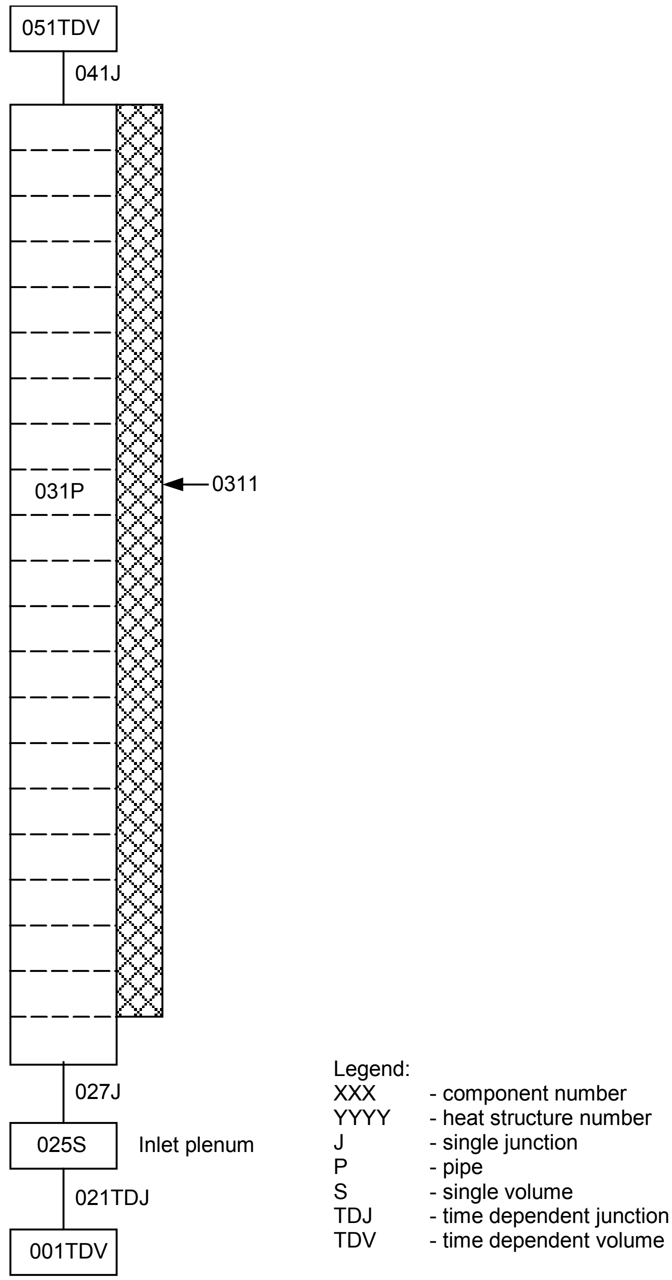

Figure 4. General nodalization of the EREC bundle models.

200 s; the rate of increase was 0.5 kW/s or smaller. The outlet pressure and initial power were then iterated until CHF occurred during the calculation at the appropriate bundle inlet pressure.

Similar input decks were used for the INEEL analysis of all three sets of experiments. The basic nodalization is shown in Figure 5. A time dependent volume and junction at the bottom of the bundle established the inlet flow and temperature. The single junction and time dependent

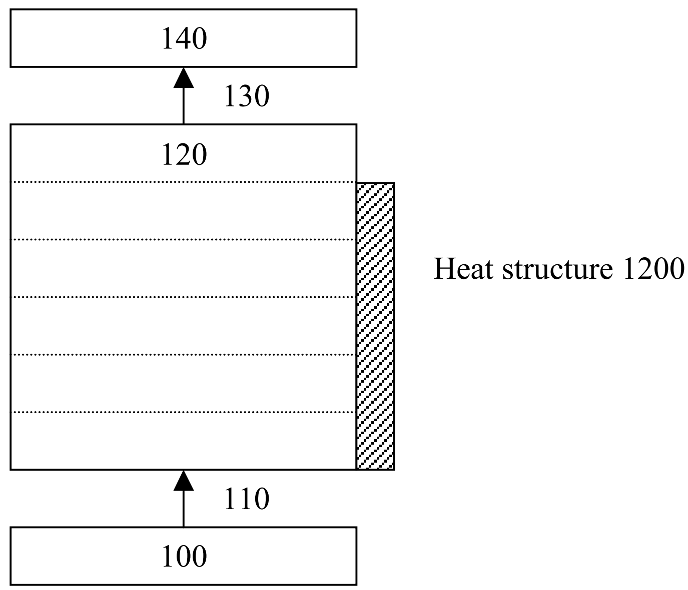

Figure 5. General nodalization of the INEEL bundle models.

volume at the top of the bundle established the pressure. The bundle region was modeled with a pipe, with the number of volumes changing for each facility. A heat structure was used to model the heater rods, with a one-for-one axial nodalization correspondence with the hydraulic volumes over the heated length, with an unheated volume at the top of the bundle. The outer wall of the bundle was not included in the base nodalization because the data provided were for the net heat flux, that is the power input minus the heat loss.

For the 4/- bundle in the KS-1 facility, the pipe had twelve 0.24-m high cells, with 11 of the cells spanning the heated length. For the 3/- bundle in the KS-1 facility, the pipe had eleven 0.25-m high cells, with 10 of the cells spanning the heated length. The junctions between the cells were aligned with the grid spacers in both of these models. Grid spacer loss coefficients of 0.5 were used in the heat structures only.

For the 7-rod bundle in the V-200 facility, the pipe had nine 0.10-m high cells, with eight of the cells spanning the heated length. Three grid spacers were modeled, at 0.2, 0.6 and 0.8 m above the bottom of the heated region. Grid spacer loss coefficients of 0.1 were used in the heat structure only.

The heater rods were modeled as cylindrical heat structures with four mesh points. The vertical rod bundle without crossflow heat transfer package was used. The hydraulic diameters were used for the heated diameters: 8.43 mm for the KS-1 4/- bundle, 8.24 mm for the KS-1 3/- bundle, and 6.46 mm for the V-200 bundle.

Default code options were used for all of the junctions and volumes, except for setting the bundle flag to 1 in the pipe; this enables the bundle interphase drag correlation.

For each test point, the inlet temperature and flow were set using the inlet time dependent volume and junction, respectively. The pressure in the outlet time dependent volume was set to provide the desired pressure at the inlet of the bundle. The power was held constant for a short period (5 – 40 s) to allow subcooled, steady state conditions to be established, then the power input to the heater rods was steadily increased until CHF occurred. After the calculation, this pressure was checked. If the pressure was not at the desired value, the outlet pressure was adjusted, and the transient calculation re-run, until the desired inlet pressure was achieved.

Results

The test series with the KS-1 37-rod bundle 4/- included 63 data points at varying pressures, temperatures, and flow rates. A comparison of the base case calculated results of EREC and INEEL for this bundle is presented in Figure 6. This figure shows deviations between the measured CHF and values calculated by EREC and INEEL for all data points of the bundle 4/- test series. The deviations are defined as:

$$\text{Deviation (\%)} = \frac{\text{CHF}_{\text{measured}} - \text{CHF}_{\text{calculated}}}{\text{CHF}_{\text{measured}}} \times 100.$$

All of the measured CHF values were overpredicted by the code in both teams' calculations.

The predictions were generally worse at low pressure and higher mass flux, with no apparent dependence on the inlet water temperature or subcooling. The pressure was a more dominant influence than the mass flow.

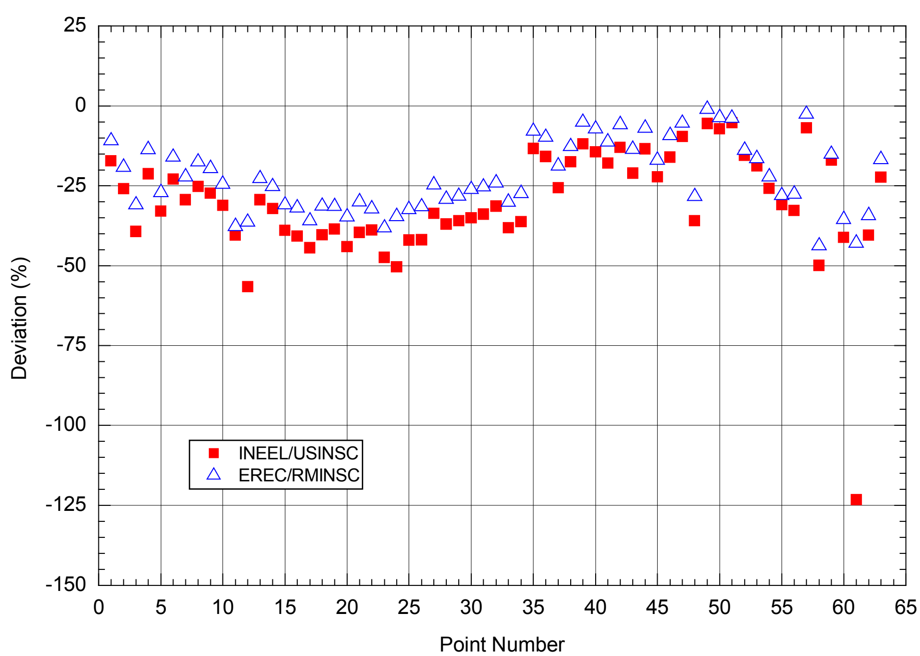

Figure 6. Comparison of the calculated results of EREC and INEEL for the KS-1 bundle 4/-.

The test series with the KS-1 19-rod bundle 3/- included 54 data points at varying pressures, temperatures, and flow rates. A comparison of the base case calculated results of EREC and INEEL for this bundle is presented in Figure 7. This figure shows deviations between the measured CHF and values calculated by EREC and INEEL for all data points of the bundle 3/- test series.

All of the measured CHF values were overpredicted by the code in both teams' calculations. Both teams found that the deviation depends on the pressure. The larger deviations were at lower pressures. In both cases, these calculations had larger deviations than the 37-rod bundle tests, because there were more points at low pressure, where the code is overpredicting the CHF by a larger margin than at high pressures. There was no apparent dependence on the mass flux. As for the 37-rod bundle, there was no apparent dependence in the calculated heat flux based on the inlet fluid temperature or subcooling.

The test series with the V-200 7-rod bundle included 25 data points at the same pressure, with varying temperatures and flow rates. A comparison of the base case calculated results of EREC and INEEL for this test series is presented in Figure 8.

All of the measured CHF values were overpredicted by the code in the INEEL base case calculations. In the EREC base case calculations, three points were slightly underpredicted; the others were overpredicted. In both teams' calculations there was a noticeable effect of mass flux on the predicted CHF, with the overprediction being greater at higher mass fluxes.

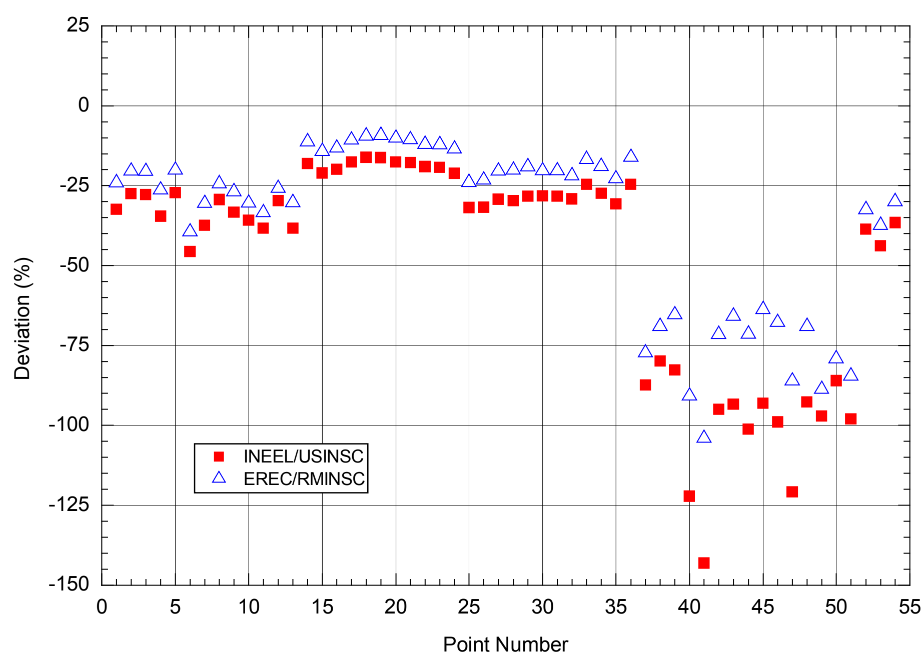

Figure 7. Comparison of the calculated results of EREC and INEEL for the KS-1 bundle 3/-.

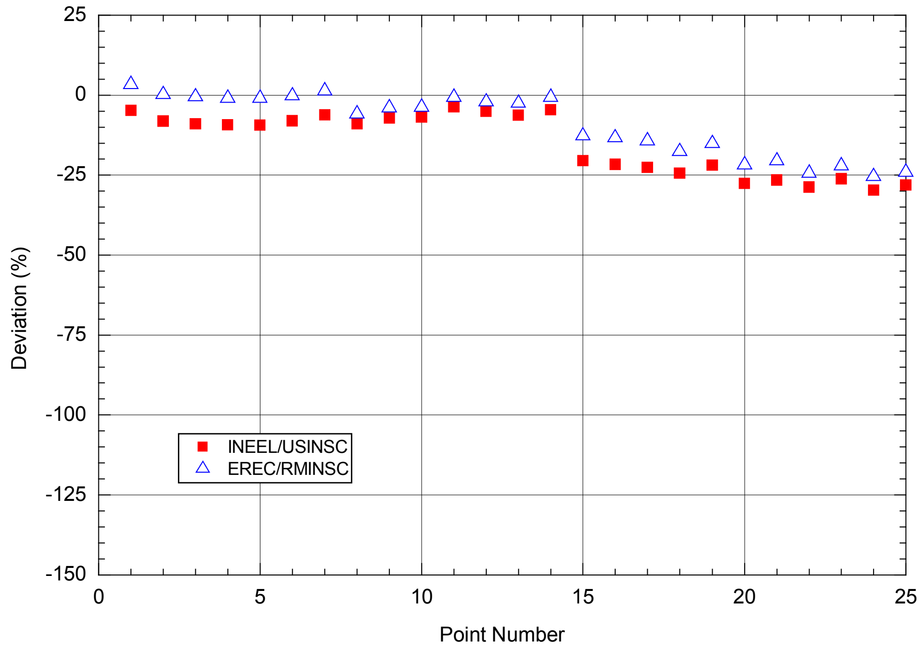

Figure 8. Comparison of the calculated results of EREC and INEEL for the V-200 bundle.

In both teams' calculations there was no noticeable effect of inlet subcooling on the predicted CHF for the lower mass flux cases. For the higher mass flux cases the deviation decreases with increasing water subcooling.

All CHF values calculated by the INEEL had larger calculation deviations than those of EREC.

Discussion of Differences

Two teams have independently developed input decks to analyze this standard problem. As a result there are differences between the RELAP5 models, which lead to differences in the calculated results. The differences between the calculations were generally small compared to the deviations between the calculated and measured critical heat fluxes. Sensitivity calculations were performed to determine the principal contributors to the differences in the calculated CHF.

For the KS-1 experiment series, the main differences in the models were the axial nodalization of the working channel, use of the thermal stratification model, the grid loss coefficient value in the heat structure (used for CHF calculation), and the heated equivalent diameter value. Sensitivity calculations were performed with both input models to investigate the effects of these differences on the calculated CHF for KS-1 bundle 3/- point 54. The approach was to change the parameters in each input deck to the value used in the other input deck. For example, the EREC base model had 20 axial nodes over the heated length, and the INEEL model had 10. For the first sensitivity calculation, the EREC model was changed to 10 axial nodes and the INEEL model to 20.

Each of the individual modeling changes increased the CHF calculated with the EREC model and decreased the CHF calculated with the INEEL model, moving the CHF values closer together. The axial nodalization and the grid spacer loss coefficient changes yielded about equal changes in the CHF in both models, while changing the heated diameter had a larger effect on the EREC model. Turning the thermal front tracking model on in the INEEL model led to large mass errors in the calculations, ranging from 13-19% of the bundle coolant mass. These large losses of coolant, in an experiment in which it is coolant depletion that causes the CHF, render these calculations highly questionable. With all of the modeling changes included, the sensitivity calculations were very close to the other model's base calculation. This shows that there are not other modeling differences that are unaccounted for.

Both teams' RELAP5 models for the V-200 experiments had the same nodalization of the working channel. In contrast to the KS-1 case, the thermal stratification model did not have a significant impact on the calculated results, and large mass errors were not observed. Two parameters had a significant influence on the calculated results, the heated equivalent diameter and the elevation of the middle grid spacer (the closest one upstream of the CHF location). As for the KS-1 3/- bundle, this shows that there are not other modeling differences that are affecting the CHF calculation.

Conclusions and Recommendations

Overall, the agreement between RELAP5/MOD3.2 calculations and the experiment results is judged to be minimal. The CHF was overpredicted in nearly every case. For the V-200 test series at low mass flux, the calculations were within the uncertainty band of the data, which is reasonable or excellent agreement. However, the calculations were outside the stated uncertainty for most of the other tests. While the value of the CHF was not predicted well, the cause was (dryout at the top of the heated channel). These assessments indicate that a CHF model more applicable to the VVER core geometry is needed in the RELAP5/MOD3.2 code.

There was no evidence of a bundle size effect. The code CHF predictions were generally worse at low pressure. Deviations at moderate and high pressures were comparable between these test series.

This assessment shows that the code generally overpredicts CHF in the hexagonal geometry typical of VVER cores. There is no way that the user can work around this problem through input. If the occurrence of CHF is important to the analysis, a side calculation can be performed by using control variables and an appropriate correlation. Although this will not affect the model response, it will tell the user if and when CHF would occur if a different model were in the code. The assessment results also serve as a reminder that it is the user's responsibility to make sure that the models in the code are being applied within their range of applicability.

Some insight into plant modeling may be gained by examining the input model differences, since there were differences in the calculated results for the two teams. Most of the differences in the input models were the result of uncertainty in the geometry or flow characteristics (loss coefficients) in the experiments. For a plant, the geometry would be better defined. Care should be taken that the grid spacer locations are input accurately, as they affect the CHF calculation (as seen in the V-200 sensitivity calculations). Given that the geometry is known, the remaining differences in the models were the axial nodalization for the KS-1 facility and the use of the thermal front tracking model.

Increasing the axial nodalization in the KS-1 sensitivity calculation improved the prediction, but the change was only a small fraction of the deviation from the measured CHF. There are also tradeoffs for the user to consider when looking at finer nodalizations. Besides the additional nodes slowing the calculation and creating larger output files, the smaller length of the nodes may result in the Courant limit being reduced, which could significantly increase the run time of the plant calculations.

The thermal front tracking model should not be used in a heated channel. This model was developed to prevent numerical diffusion in large tanks in which cold water flowing out the bottom of the vessel is replaced by hot water entering the top. Many of the calculations with the model turned on had large enough mass errors that the validity of the calculations would be questioned.

References

1. The RELAP5 Code Development Team, "RELAP5/MOD3 Code Manual", NUREG/CR-5535 (INEL-95/0174), Volumes I-V, Idaho National Engineering Laboratory, Idaho Falls, Idaho (June 1995).
2. L. L. Kobzar, R. S. Pomet'ko, and M. V. Davydov, "Standard Problem INSCSP-V7 Definition Report: VVER Core Heat Transfer" (Deliverable V7-1 of Work Order 984216426 under Joint Project 6 with the U. S. International Nuclear Safety Center), International Nuclear Safety Center of Russian Minatom (June 2000).
3. M. V. Davydov and O. I. Melikhov, "Final Analysis Report for Standard Problem INSCSP-V7: VVER Core Heat Transfer" (Deliverable V7-3 of Work Order 984216426 under Joint Project 6 with the U. S. International Nuclear Safety Center), International Nuclear Safety Center of Russian Minatom (July 2001).
4. Paul D. Bayless, "RELAP5/MOD3.2 Assessment Using CHF Data from the KS-1 and V-200 Experiment Facilities", INEEL/EXT-01-00782, Idaho National Engineering and Environmental Laboratory (July 2001).